

# Corrosion Behavior of Thermally Sprayed WC Coating in Na<sub>2</sub>SO<sub>4</sub> Aqueous Solution

Mutsumi Takeda<sup>1,\*</sup>, Naoki Morihira<sup>1,\*</sup>, Ryuichiro Ebara<sup>2</sup>, Yoshio Harada<sup>3</sup>,  
Rongguang Wang<sup>1</sup> and Mitsuo Kido<sup>1</sup>

<sup>1</sup>Hiroshima Institute of Technology, Hiroshima 731-5193, Japan

<sup>2</sup>Faculty of Engineering, Kagawa University, Takamatsu 761-0396, Japan

<sup>3</sup>Tocalo Co., Ltd., Kobe 658-0013, Japan

WC-Co thermally sprayed coating, formed by high velocity oxygen-fuel flame spraying, has had the problem of low corrosion resistance in aqueous solutions. Furthermore, much remains unknown regarding corrosion reactions on coating surfaces and the formation of passivation films. This study focused on changes of the corrosion surfaces of two thermally sprayed coatings, WC-12Co and WC-10Co-4Cr, with immersion time. The chemical composition of the corrosion surfaces was analyzed by electron spectroscopy, and the relation with passivation film stability is discussed. For WC-12Co, the thermally sprayed coating was immersed in Na<sub>2</sub>SO<sub>4</sub> solution. The W and Co components were dissolved by extended anodic reaction. Oxides of W and Co were then formed on the surface of the thermally sprayed coating. However, these oxides appeared to have little effect on the corrosion. Passivation film, which mainly consists of Cr<sub>2</sub>O<sub>3</sub>, was formed on the surface of WC-10Co-4Cr thermally sprayed coating immediately after immersion, and limited the dissolving of coating components into the aqueous solution. However, it is suspected that this film did not completely cover the entire coating surface. It is probably a thin porous film formed as islands.

(Received May 23, 2002; Accepted September 24, 2002)

**Keywords:** thermally sprayed coating, high velocity oxygen-fuel flame spray, tungsten carbide cermet coating, passivation film, immersion, corrosion resistance, anodic polarization

## 1. Introduction

WC coatings thermally sprayed by high velocity oxygen-fuel flame (HVOF) are widely used in many industries because of their high wear resistance.<sup>1-3)</sup> However, their uses are limited by their poor corrosion resistance, though many efforts to improve WC-Co coatings<sup>4-7)</sup> have been reported. In order to solve this problem, it is necessary to investigate their corrosion behaviors,<sup>8)</sup> including passive film formation<sup>9)</sup> in corrosive solutions, but to date, these have not been elucidated.

The authors previously reported the corrosion behaviors of WC-Co and WC-Co-Cr sprayed coating in Na<sub>2</sub>SO<sub>4</sub> aqueous solutions, including anode polarization and impedance response.<sup>10)</sup> The corrosion resistance of WC-Co-Cr coating was found to be higher than that of WC-Co coating, which might have resulted from an easily formed passive film containing chromium. However, the passive film has not been investigated.

In this study, the potential distributions of the two thermally sprayed coatings, WC-12Co and WC-10Co-4Cr, were measured in Na<sub>2</sub>SO<sub>4</sub> aqueous solutions. Corrosion products were analyzed by Electron Spectroscopy for Chemical Analysis (ESCA). The relation between surface composition and passive film stability is discussed.

## 2. Experimental Methods

### 2.1 Specimens and solutions

Two types of composite powders (agglomerated-sintering) of WC-12 mass% Co and WC-10 mass% Co-4 mass% Cr

were used as HVOF thermally sprayed material. The substrate was SS400 steel with a cylindrical form ( $\phi$ 19 mm  $\times$  10 mm), and the sprayed coating thickness was about 200  $\mu$ m. The chemical compositions of substrate and powder are shown in Tables 1 and 2, respectively. The coating surfaces were first polished by emery paper (#800), then ultrasonically cleaned in acetone for 1.8 ks before the corrosion test. The corrosion test area was approximately  $1.0 \times 10^2$  (mm<sup>2</sup>).

0.05 kmol/m<sup>3</sup> Na<sub>2</sub>SO<sub>4</sub> aqueous solutions were used in corrosion tests with pH values adjusted by H<sub>2</sub>SO<sub>4</sub> and NaOH. Air or nitrogen was blown into the solution for 3.6 ks to examine the influence of dissolved oxygen. All solutions were kept at  $323 \pm 1$  K.

### 2.2 Polarization and potential static tests

The anodic polarization curves were measured with a potentiostat apparatus, where Pt was the counter electrode, and a saturated calomel electrode (S.C.E.) was the reference electrode.

Table 1 Chemical compositions of substrate.  
(mass%)

Substrate	C	Si	Mn	P	S
SS400 (JIS)	0.14	0.14	0.59	0.033	0.032

Table 2 Chemical compositions of powder.  
(mass%)

Powder	W	Co	Cr	C	Fe
WC-12Co	Bal.	11.90	—	5.33	0.09
WC-10Co-4Cr	Bal.	9.80	3.04	5.27	0.20

\*Graduate Student, Hiroshima Institute of Technology.

### 2.3 Surface analysis by ESCA

The surfaces were analyzed with ESCA (SHIMADZU Co. Ltd: AXIS-ULTRA) after natural immersion and potentiostatic immersion in Na<sub>2</sub>SO<sub>4</sub> solutions open to the atmosphere. The potentiostatic immersion tests were carried out using the potentiostat after keeping it at the natural potential for 1.2 ks. The applied potentials in the potentiostatic test were taken from previous data. The potentiostatic or natural immersion was carried out for 1.8 ks.

After polarization and immersion, specimens were ultrasonically cleaned in acetone for 1.8 ks, and put into the ESCA chamber as quickly as possible. In this analysis, Mg was used to produce X-rays, and the air pressure in the vacuum chamber was 10<sup>-6</sup>–10<sup>-7</sup> Pa. The specimen surfaces were etched by Ar<sup>+</sup> to obtain depth information.

### 2.4 Scanning vibrating electrode technique test

The potential distributions on specimen surfaces immersed in Na<sub>2</sub>SO<sub>4</sub> solution at open circuit were measured using scanning vibrating electrode apparatus (HOKUTODENKO Co. Ltd: SVET HV-301). The vibrating electrode was made of Pt with a tip diameter of 20 μm. The specimens for this test were polished by emery paper (#800) and diamond powder (average diameter: 3 μm). The distance between the electrode and the sample surface was set at 10 μm (constant) and the scanning area was 1.5 mm<sup>2</sup>.

## 3. Results and Discussion

### 3.1 Anodic polarization characteristic

Figure 1 shows the anodic polarization curves for WC-12Co and WC-10Co-4Cr (hereinafter Co-Coating and Cr-Coating) coating specimens in Na<sub>2</sub>SO<sub>4</sub> solutions at pH = 6.5. The current density *I* of the Co-Coating in the passive region (*E* = 0.1–0.5 V) was higher than that of the Cr-Coating. A similar result was obtained at pH = 12.0. Passive film containing Cr might be produced on the Cr-Coating, which displays high corrosion resistance, though current density gener-

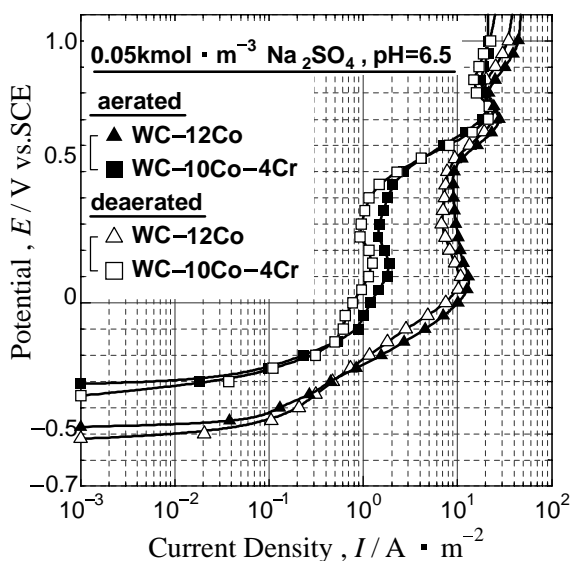


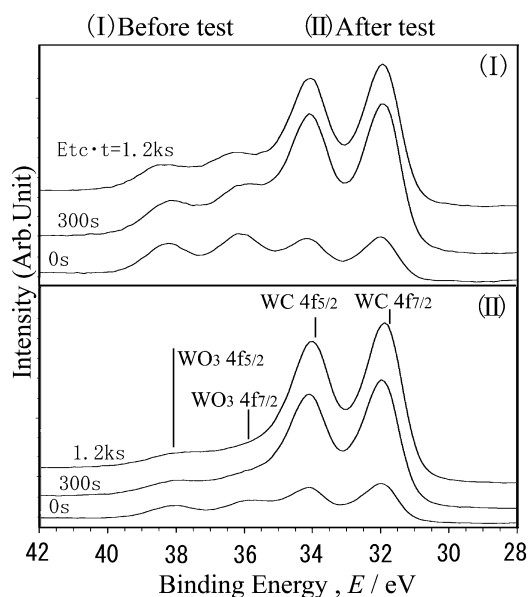
Fig. 1 Polarization curves of WC-Co thermally sprayed coatings in 0.05 kmol·m<sup>-3</sup> Na<sub>2</sub>SO<sub>4</sub> solution.

ally increases because WC and Co can easily be dissolved in neutral and alkaline solutions.<sup>10)</sup> Moreover, the passive current density was lower under deaerated test conditions.

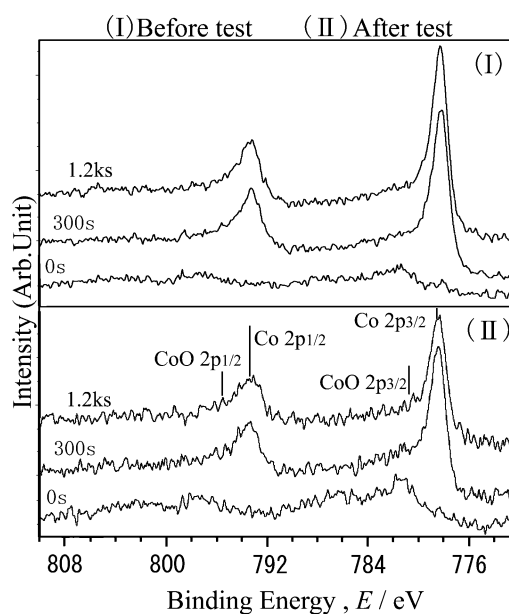
### 3.2 Surface composition analysis before and after anodic polarization by ESCA

The surface composition of both Co and Cr coatings was immediately analyzed by ESCA after potential static test on the passive state area (*E* ≈ 0.3 V) in a solution. The results in Fig. 2 show the spectra before ((I)) and after ((II)) testing. The subscripts to the left indicate etching time (Etc·t) by Ar<sup>+</sup> in ESCA analysis.

Photoelectron peaks appeared at about 32 eV and 34 eV be-



(a) W 4f spectra



(b) Co 2p spectra

Fig. 2 Analysis results (spectra) before corrosion and after potential static test (*E* ≈ 0.3 V) for WC-12Co thermally sprayed coating with ESCA in 0.05 kmol·m<sup>-3</sup> Na<sub>2</sub>SO<sub>4</sub> solution. (Etc·t: Etching time) (a) W 4f spectra (b) Co 2p spectra.

fore and after corrosion of the Co-Coating, corresponding to WC  $4f_{7/2}$  and WC  $4f_{5/2}$  respectively.<sup>11,14)</sup> There was no large difference between them before and after corrosion. Two weak peaks also appeared at about 36 eV and 38 eV before and after corrosion, corresponding to  $WO_3$   $4f_{7/2}$  and  $WO_3$   $4f_{5/2}$  respectively. The intensity of the two weak peaks decreased remarkably after  $Ar^+$  etching, and they almost disappeared after  $Etc \cdot t = 1.2$  ks. Accordingly, the oxidation film on W might be thin.

According to Co 2p spectra (Fig. 2(b)), their shapes were almost the same before and after test. Two peaks appeared at about 780 eV and 796 eV corresponding to CoO  $2p_{3/2}$  and  $2p_{1/2}$  peaks. Two other strong peaks matched Co  $2p_{3/2}$  and Co  $2p_{1/2}$  and appeared at about 778 eV and 793 eV after  $Ar^+$  etching. Their intensities were almost the same between spectra after  $Etc \cdot t = 300$  s and 1.2 ks because the contamination and oxide layer on the surface after  $Ar^+$  etching might be removed. The strong peaks that appeared after etching were thought to be oxide or hydroxide.

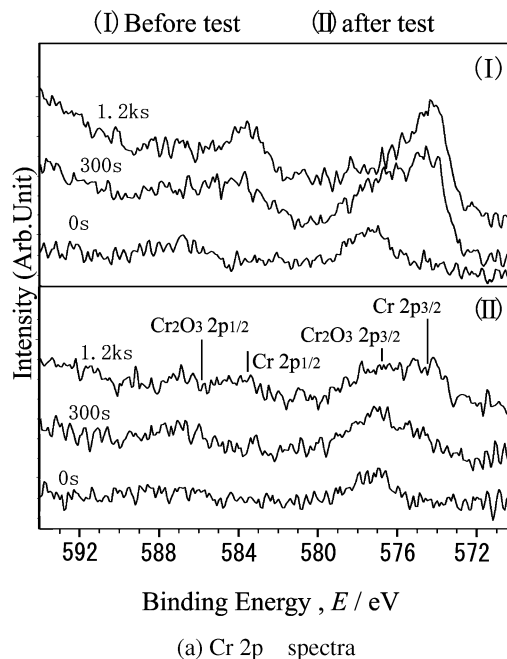
W 4f spectra ( $WO_3$   $4f_{7/2}$  and  $WO_3$   $4f_{5/2}$ ) of the Cr-Coating also appeared before and after corrosion, nearly repeating the results of the Co-Coating. Two Cr 2p peaks appeared at about 577 eV and 587 eV near the outermost surface of all the specimens on Cr-Coating before and after testing, shown in Fig. 3(a). These corresponded to the peaks for  $Cr_2O_3$   $2p_{3/2}$  and  $2p_{1/2}$ .<sup>8,11-13)</sup> Accordingly,  $Cr_2O_3$  was present before corrosion of the Cr-Coating surface. Although the amount of  $Cr_2O_3$  on the surface before corrosion decreased greatly after etching ( $Etc \cdot t = 300$  s), it was strong after  $Etc \cdot t = 1.2$  ks after test. This finding suggests that a thick oxidation film of Cr was generated on the surface after corrosion because the metal peak of Cr did not appear as clearly as before corrosion.

Figure 3(b) shows Fe 2p spectra before and after testing. Fe was not detected on the surface before testing, while peaks for Fe  $2p_{3/2}$  and  $2p_{1/2}$ <sup>11,12)</sup> appeared at 711 eV and 724 eV after corrosion. The peaks were characteristic of FeO and  $Fe_2O_3$ . It will be necessary to determine whether a small amount of Fe present in the coating or in the substrate (SS400) might have oxidized and dissolved.

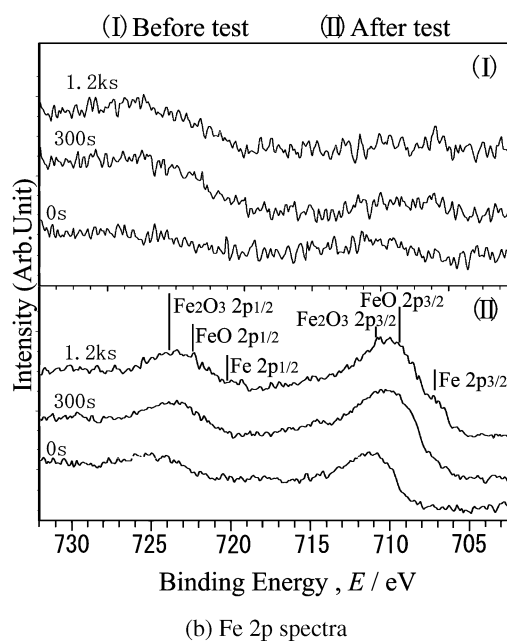
### 3.3 Surface potential distribution during immersion

According to the ESCA analysis after polarization measurement in Section 3.2, the formation of oxides and hydroxides was confirmed on coating surfaces. In this section, potential distribution in  $Na_2SO_4$  aqueous solution (pH = 6.5) was investigated with the scanning vibrating electrode apparatus. The results are shown in Figs. 4 and 5. Plus values on the vertical axis show anodic reactions while minus values show cathodic reactions. The average values of potential with immersing time are shown in (a)', (b)' and (c)', respectively. The horizontal axis means the position in the Y direction.

In the case of the Co-Coating specimen (Fig. 4), all the measured area showed anodic reaction, meaning corrosion on initial immersion (Fig. 4(a)). Potential values gradually decreased with probe scanning in the Y direction, indicating that the corrosion reaction weakened over time. With immersion time increased to  $t_i = 36$  ks (Fig. 4(b)), anodic reaction became much weaker. The initial anodic reaction might be due to surface activation by polishing. The cathodic area increased as surfaces were covered with corrosion products (ox-



(a) Cr 2p spectra



(b) Fe 2p spectra

Fig. 3 Analysis results (spectra) before corrosion and after potential static test ( $E \approx 0.3$  V) for WC-10Co-4Cr thermally sprayed coating with ESCA. (a) Cr 2p spectra, (b) Fe 2p spectra.

ides or hydroxides) over the immersion time.

In the case of the Cr-Coating specimen (Fig. 5), intense local anodic and cathodic reactions existed simultaneously after immersion. The intense anodic reaction then disappeared, and weak anodic and cathodic reactions existed simultaneously after 36 ks immersion. The reaction tendencies were almost unchanged, though the surface potential distributions changed after 90 ks immersion. Accordingly, in the case of the Cr-Coating specimen mentioned in Section 3.2, the anodic reactions would become weaker because a passive film of  $Cr_2O_3$  was formed in the initial immersion when local anodic reactions were intense. Given the above, the passive film containing  $Cr_2O_3$  might not be a uniform layer but a porous set of islands on the surface.

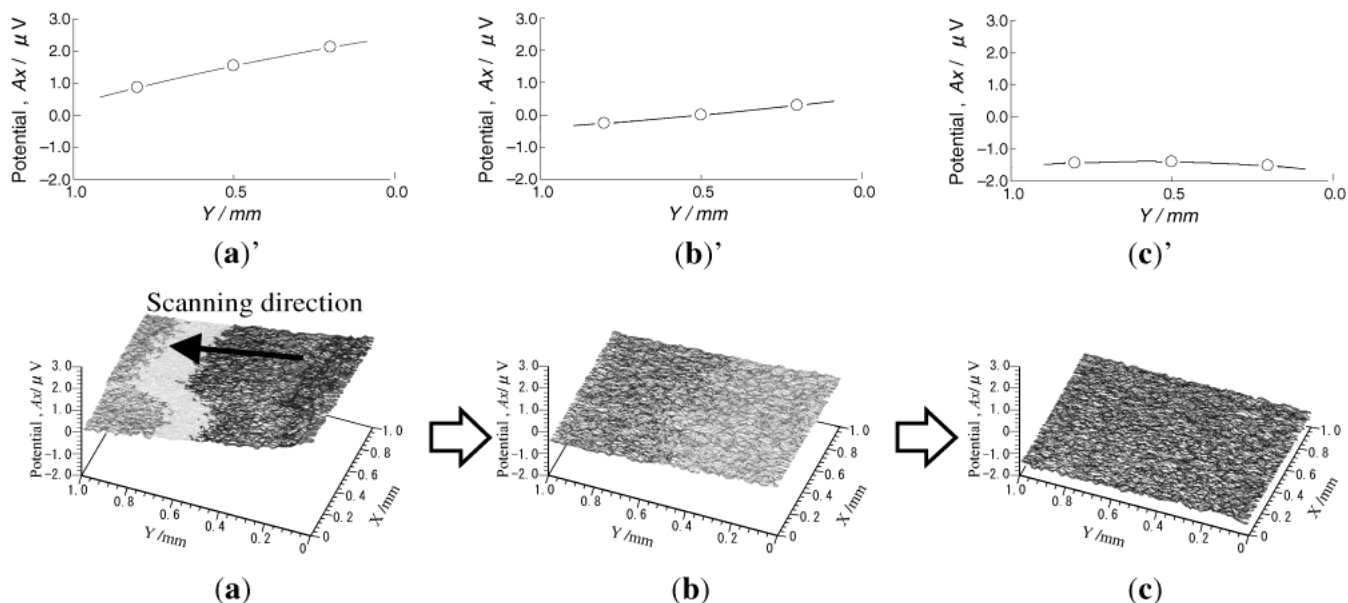


Fig. 4 Change of potential distribution with immersion time  $t_1$  for WC-12Co coating. (a), (a)':  $t_1 = 0.6$  ks (b), (b)':  $t_1 = 36$  ks (c), (c)':  $t_1 = 90$  ks.

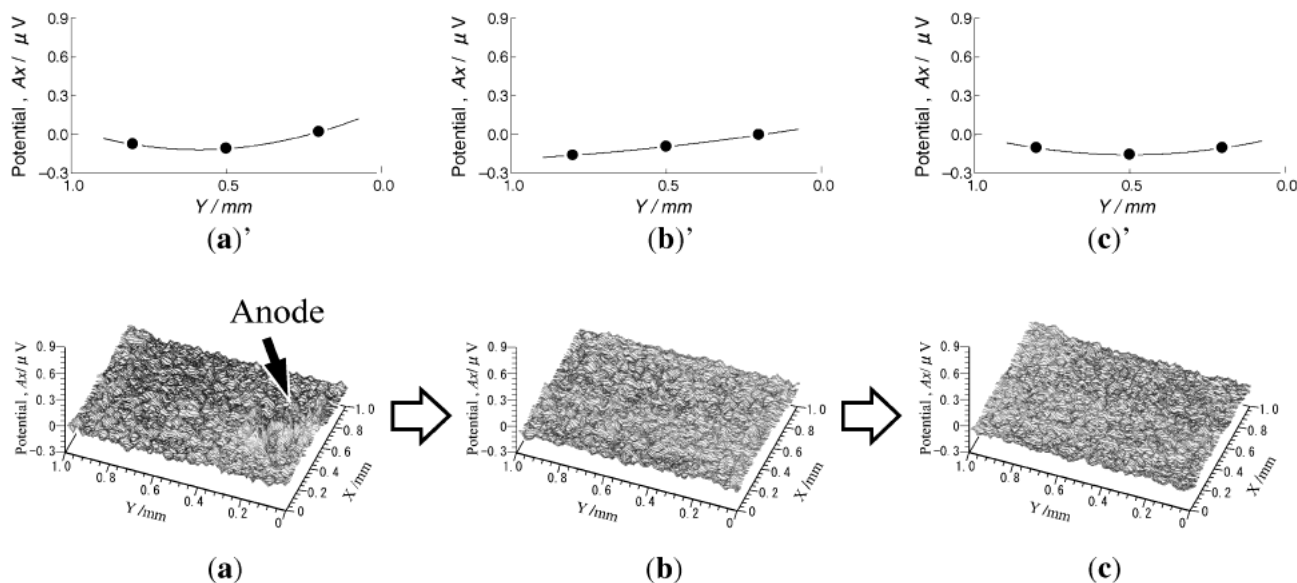


Fig. 5 Change of potential distribution with immersion time  $t_1$  for WC-10Co-4Cr coating. (a), (a)':  $t_1 = 0.6$  ks (b), (b)':  $t_1 = 36$  ks (c), (c)':  $t_1 = 90$  ks.

### 3.4 ESCA surface composition analysis after immersion

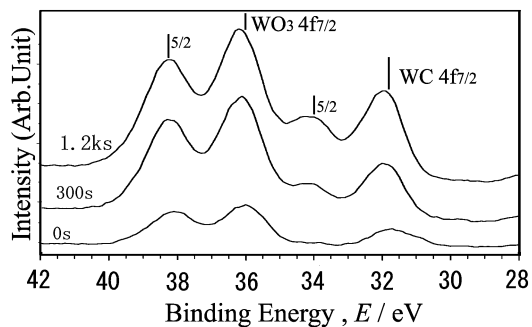
The surfaces were immediately analyzed by ESCA after natural immersion for  $t_1 = 86.4$  ks in order to investigate surface composition changes due to immersion.

Figure 6(a) shows the W 4f spectra of Co-Coating. Although the peaks of WC  $4f_{7/2}$  and WC  $4f_{5/2}$  appeared similar to those before corrosion, as shown in Fig. 2(a), their intensities largely decreased dramatically after immersion and almost disappeared on the outermost surfaces. These results were confirmed after  $t_1 = 43.2$  ks natural immersion. On the other hand, the amount of WO<sub>3</sub> increased. Accordingly, large amounts of oxides had been formed on the surface after immersion in Na<sub>2</sub>SO<sub>4</sub> solution.

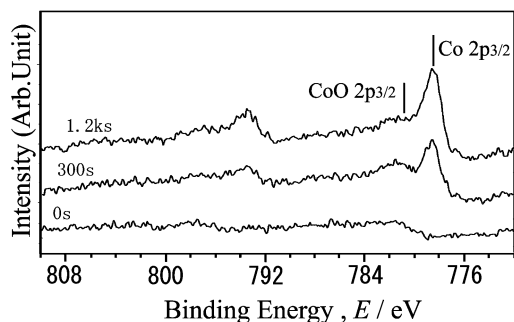
According to Co 2p spectra (Fig. 6(b)), the CoO peak ap-

peared on the outermost surface of the coating, and a peak from metallic Co appeared after Etc  $\cdot t = 300$  s. CoO was still present after Etc  $\cdot t = 1.2$  ks, suggesting that more oxide formed during immersion rather than before immersion. Accordingly, the gradual corrosion potential shifting from the initial anodic reaction to the cathodic reaction mentioned in section 3.3 might have resulted from the formation of WO<sub>3</sub>, CoO, FeO and Fe<sub>2</sub>O<sub>3</sub> on the surface.

On the other hand, the spectra of W and Co of Cr-Coating hardly changed after natural immersion. Considering that the intensity of the Cr<sub>2</sub>O<sub>3</sub> peak in the Cr 2p spectra shown in Fig. 7 was still high after Etc  $\cdot t = 300$  s, a passive film containing more Cr<sub>2</sub>O<sub>3</sub> might have formed after immersion, which would suppress the dissolving of W and Co.



(a) W 4f spectra



(b) Co 2p spectra

Fig. 6 Analysis results (spectra) for WC-12Co thermally sprayed coating with ESCA. (Immersion time  $t_1 = 86.4$  ks) (a) W 4f spectra, (b) Co 2p spectra.

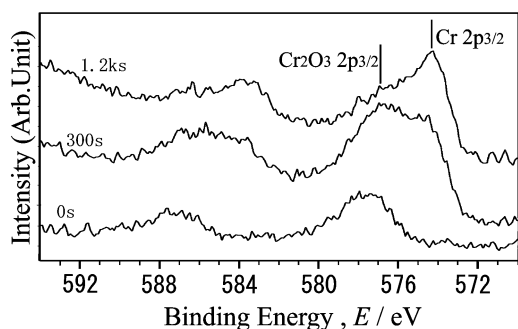


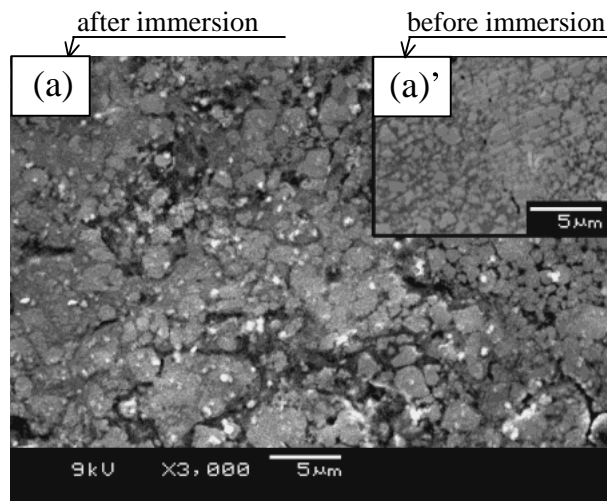
Fig. 7 Analysis results (Cr 2p spectra) for WC-12Co thermally sprayed coating by ESCA. (Immersion time  $t_1 = 86.4$  ks).

### 3.5 Surface morphologies and composition change by immersion

The surface morphologies after 86.4 ks immersion observed by SEM are shown in Figs. 8(a) and (b). The surface morphologies before immersion are shown in (a') and (b'). In the case of the Co-Coating specimen, compared with the appearance before immersion, the surface appears to be extremely uneven island shapes. The WC (main composition) grain boundary can be clearly observed, which might be attributed to the resolution of Co (combination phase). On the other hand, the resolution of Co on the surfaces of Cr-Coating specimen cannot be precisely known, though the surface was also somewhat uneven.

In the case of the Co-Coating specimen described in Fig. 9, the coating before immersion was composed of WC grains and combination phase Co, with small amounts of  $WO_3$  and CoO on the surfaces. For more oxides ( $WO_3 > CoO$ ) were

#### WC-Co coating



#### WC-Co-Cr coating

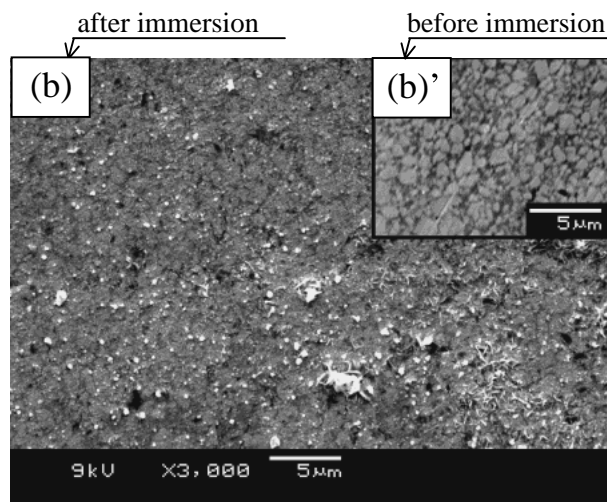


Fig. 8 SEM surface micrographs of thermally sprayed coating before and after immersion in  $Na_2SO_4$  solution. (a) WC-12Co after 86.4 ks immersion, (a') WC-12Co before immersion, (b) WC-10Co-4Cr after 86.4 ks immersion, (b') WC-10Co-4Cr before immersion.

formed and covered the surfaces after immersion.  $WO_3$  dissolved to become  $WO_4^{2-}$ , which was then redeposited on the specimen surface because it does not dissolve well in water. CoO dissolved to  $Co^{2+}$ , which can be combined with water to form CoO again, and also redeposited on the specimen surface.<sup>6)</sup> However, these deposited oxides show no ability to reduce the corrosion rate, resulting in the rapid further dissolution of the sprayed composition. In fact, the island phenomenon appeared because of the rapid dissolving of Co. On the Cr-Coating specimen shown in Fig. 10, the coating structure was almost the same as the Co-Coating specimen before immersion.  $WO_3$  and  $Cr_2O_3$  were present on the surface. Suppression by  $Cr_2O_3$  was confirmed because the surface changed only slightly after immersion. However, the corrosion suppression was not complete. Small amounts of W and Co were still dissolved. According to the above potential distribution measurement, the distribution of oxides on the surface was unstable and not uniform, meaning that parts of

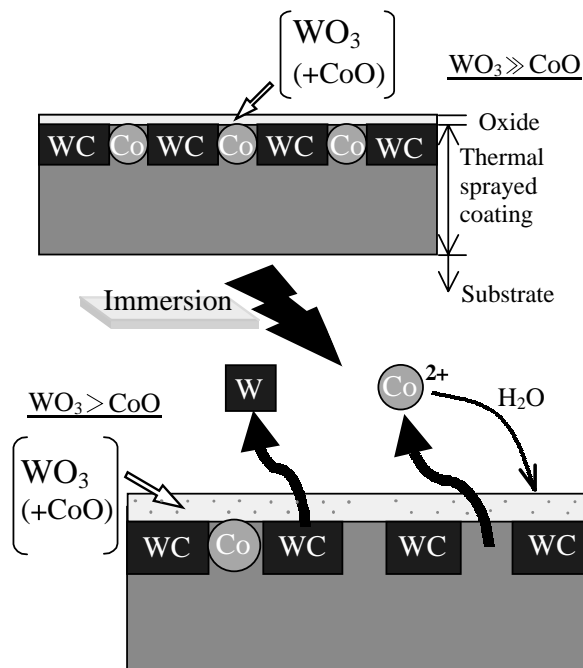


Fig. 9 Schematic illustration of WC-12Co thermally sprayed coating before and after immersion in Na<sub>2</sub>SO<sub>4</sub> solution.

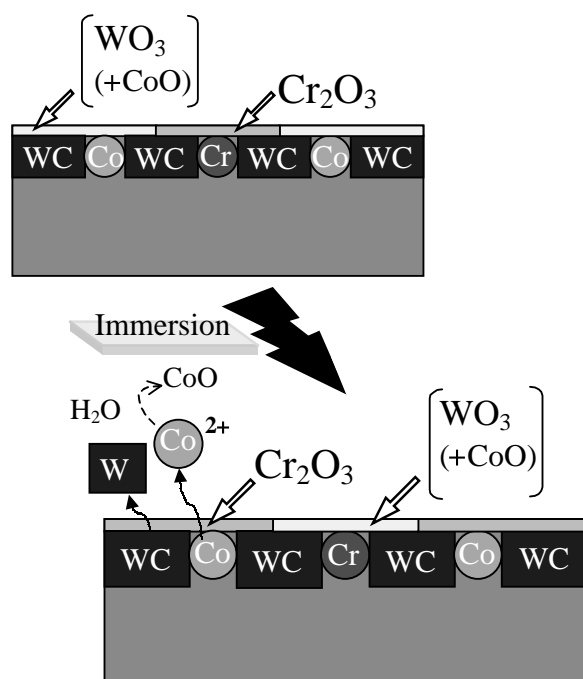


Fig. 10 Schematic illustration of WC-10Co-4Cr thermally sprayed coating before and after immersion in Na<sub>2</sub>SO<sub>4</sub> solution.

the film islands were cyclically dissolved and reformed.

The peak intensity of WC decreased dramatically after immersion, according to ESCA analysis, while most WC particles were observed by SEM. This difference was attributed to the ESCA thickness being less than 1  $\mu$ m.

#### 4. Conclusions

Corrosion behaviors of WC thermally sprayed coating surfaces formed with HVOF were investigated, when they were immersed in aqueous solutions of Na<sub>2</sub>SO<sub>4</sub>, including the variation of surface composition with immersion time. The compounds generated on the sprayed coating surface were measured by ESCA.

The obtained results are as follows:

(1) The corrosion rate of WC-10Co-4Cr sprayed coating decreased sharply due to the formation of a thin film containing Cr<sub>2</sub>O<sub>3</sub> on the surface.

(2) Oxides or hydroxides of W and Co formed on the WC-12Co surface because WC and Co were dissolved after natural, long-term immersion in Na<sub>2</sub>SO<sub>4</sub> solution, and their ability to suppress corrosion is weak.

(3) Passive film consisting of Cr<sub>2</sub>O<sub>3</sub> formed on the surface of the WC-10Co-4Cr coating after immersion, which suppressed the dissolving of coating components in aqueous solution. However, it is suspected that this film does not completely cover the coated surface. It is probably a thin porous film formed as islands.

#### REFERENCES

- 1) A. Hasui: *Thermal Spray engineering*, (Sanpo Pub, Japan, (1996) pp. 209–259.
- 2) Y. Harada: *Bulletin of the Japan Institute of Metals* **31** (1992) 413–421.
- 3) Japan Thermal Spraying Society: *Spray technique Handbook* (1996).
- 4) K. Tani: *Thermal Spray Tech.* **9** (1990) 57–67.
- 5) C. J. Li, A. Ohmori and Y. Harada: *J. Thermal Spray Technol.* **5** (1996) 69–73.
- 6) Y. Takatani, T. Tomita, K. Tani, M. Inaba and Y. Harada: *Surf. Coat. Tech.* **49** (1998) 396–400.
- 7) Y. Takatani, T. Tomita, K. Inaba and Y. Harada: *Journal of the Society of Materials Science, Japan* **48** (1999) 1249–1254.
- 8) K. Sugimoto: *Journal of the Japan Inst. Metals seminar, Journal of the Japan Institute of Metals* (1988) pp. 19–25.
- 9) K. Yoshimi and M. Kido: *Journal of the Society of Materials Science, Japan* **41** (1992) 119.
- 10) M. Takeda, T. Okabe, M. Kido and Y. Harada: *Thermal Spray*, **38** (2001) 58–64.
- 11) C. D. Wagner: *Practical Surface Analysis*, pp. 598–620.
- 12) H. Shibuya, M. Morinaga and K. Kikuchi: *J. Japan Inst. Metals* **62** (1998) 534.
- 13) J. D. Olivas, C. Mireles, E. Acosta and E. V. Barrera: *Thin Solid Films* **299** (1997) 143–148.
- 14) H. Nakahira, Y. Harada, T. Doi, Y. Takatani and T. Tomita: *Journal of High Temperature Society* **16** (1990) 317–323.